JETIR.ORG ISSN: 2349-5162 | ESTD Year : 2014 | Monthly Issue
JOURNAL OF EMERGING TECHNOLOGIES AND INNOVATIVE RESEARCH (JETIR)
An International Scholarly Open Access, Peer-reviewed, Refereed Journal

A Deep Learning Model for Blood Vessel Segmentation and Classification for Cardiovascular Diseases Detection

[1,*]R. Ramesh, [2]Dr. S. Sathiamoorthy

[1,*]Research Scholar, Department of Computer and Information Science, Annamalai University, Annamalai Nagar.
[2]Assistant Professor, Annamalai University PG Extension Centre, Villupuram. Tamilnadu.

Abstract

Cardiovascular diseases (CVDs) are a main world-wide health problem, requiring earlier diagnosis for efficient intervention. Recently, deep learning (DL) methods have been developed as robust tools for automatically diagnosing disease. This study considers leveraging DL approach for the detection of CVDs employing retinal fundus images, a non-invasive and simply available imaging modality. In this study, we present an innovative Grasshopper Optimization Algorithm with Deep Learning based Blood Vessel Segmentation and Classification (GOADL-BVSC) model for grading the CVD. This analysis suggests a robust method for CVD detection by connecting DL methodologies, particularly utilizing DenseNet for feature extraction, Grasshopper Optimization Algorithm (GOA) for parameter tuning, and Deep Belief Network (DBN) for classification. Retinal fundus images provide a useful resources for evaluating cardiovascular conditions, giving a non-invasive and quickly accessible process of detecting CVDs. DenseNet, a deep neural network (DNN) framework known for its extensive feature- representations, has been employed for extracting useful features from these images. GOA, stimulated by the foraged behavior of grasshoppers, is exploited to fine-tune the hyperparameters of the method, improving its performance. The DBN classification model is trained for differentiating among normal and CVD-affected retinal images depends on the extracted features. GOA iteratively enhances the hyperparameters of the DBN, confirming that the system attains its maximum accuracy capability. The simulation outcomes represented the excellent outcomes of the GOADL-BVSC method over other existing models with regard to different levels.

Keywords: Cardiovascular diseases; Retinal fundus images; Blood vessel segmentation; Grasshopper Optimization Algorithm; Deep learning

1. Introduction

Cardiovascular disease (CVD) is the foremost cause of death globally with type 1 and type 2 diabetes which are known high-risk issues [1]. Several struggles have been created to enhance CVD risk prediction. There is

substantial proof that retinopathy and CVD share mutual risk factors in diabetes so the analytical data on CVD may be estimated from the Retinal Images (RI) [2]. Past researchers have shown that retinal vasculature characteristics are detected by retinal fundus imaging that includes valuable info about CC health. For example, vascular calibre, venular occlusion and a combination of several retinal data have shown sturdy suggestions for the occurrence of future CC actions. In research, the people with diabetes involved quite small unit sizes [3]. This shows that there are varieties of conventional CVD risk issues like sex, age and smoking status that can be identified by employing DL on retinal fundus images. In a recent study, there was an aggressive growth in many studies that utilized AI and DL to remove data from RI [4]. The power of DL is mainly utilized to extract info from RI because there is strong interest in employing the RI data created by DL models to enhance the conventional means of assessing CVD risk [5].

Retinal photography analysis has gained huge popularity within medical imaging models due to its cost-effective nature and non-invasive [6]. Retinal fundus images (RFI) are gained from prediction of the rear portion of the eye on a two-dimensional level by utilizing a monocular camera [7]. The various eye structures and biomarkers can be recognized from RFI because it plays a vital role in detecting retinal anomalies and diseases like macular edema degeneration, diabetic retinopathy (DR), glaucoma and much more. In the last few years, DL used to ocular has stimulated abundant concern in the systematic community [8]. The prediction and identification of ocular biomarkers of general illnesses are gaining more interest from researchers [9]. DL models are producing insights regarding eye–body connections via retinal morphology examination to improve the understanding of difficult illnesses like cardiovascular disease, traumatic brain injury, renal impairment, Alzheimer's disease, musculoskeletal diseases or anaemia recognition [10].

Schlesinger and Stultz [11] developed a model to estimate DL methods and consider numerous remarkable applications in light of these rubrics. Physicians and Data scientists have similarly implemented several DL algorithms to both organized electronic health record data and medical images. In several conditions, these techniques leads to risk stratification framework, which can be enhanced discriminatory capability compared with additional straightforward techniques. Revathi et al. [12] developed Retinal fundus images to detect the possible risk influences of CVD. Hypertensive Retinopathy and Cholesterol-Embolization Syndrome (CES) have been major harmful factors. Generative Adversarial Network (GAN) was exploited as a DL technique for producing images with higher resolution. This study also employs a present retraining ImageNet architecture to solve customized image classification processes.

In [13], an efficient method for CVD risk forecast was established utilizing retinal fundus images. Firstly, pre-processing is accomplished by employing grayscale conversion. Secondly, the cardiovascular risk evaluation is performed by a Deep neuro-fuzzy network (DNFN). Lastly, the DNFN has been trained to implement the emerged Fractional Calculus-Horse Herd Optimizer Algorithm (FCHOA) that could be developed by integrating Horse Herd Optimizer algorithm (HOA) and Fractional Calculus (FC). In [14], a DL method to evaluate CACS from retinal fundus images was presented. This introduced technique executes the training of deep-CCNs (DCNNs) with retinal fundus images for forecasting auxiliary HER datasets compared with CACS. Additionally, this work performs an activity-based augmentation technique that determines flare occurrence that normally arises in a

retinal fundus image. Rim et al. [15] designed and validated an innovative cardiovascular risk stratification technique depends on DL forecasting CAC from retinal images. A DL method has been trained for forecasting the possibility of the existence of CAC such as RetiCAC, and DL retinal CAC score. This graded RetiCAC rates into tertiles and employed Cox proportional risks approach for estimative the capability of RetiCAC to prognostic CAV occurrences, which are dependent upon external testing sets.

In this study, we present an innovative Grasshopper Optimization Algorithm with Deep Learning based Blood Vessel Segmentation and Classification (GOADL-BVSC) model for grading the CVD. This analysis suggests a robust method for CVD detection by connecting DL methodologies, particularly utilizing DenseNet for feature extraction, Grasshopper Optimization Algorithm (GOA) for parameter tuning, and Deep Belief Network (DBN) for classification. DenseNet, a deep neural network (DNN) framework known for its extensive feature-representations, has been employed for extracting useful features from these images. GOA, stimulated by the foraged behavior of grasshoppers, is exploited to fine-tune the hyperparameters of the method, improving its performance. The DBN classification model is trained for differentiating among normal and CVD-affected retinal images depends on the extracted features. The simulation outcomes represented the excellent outcomes of the GOADL-BVSC method over other existing models with regard to different levels.

2. The proposed model

In this work, we have considered the development of the GOADL-BVSC method for automated and accurate CVD with retinal fundus images. The GOADL-BVSC approach includes GOA based hyperparameter tuning, DBN based classification, and DenseNet based feature extraction. Fig. 1 illustrates the entire process of GOADL-BVSC algorithm.

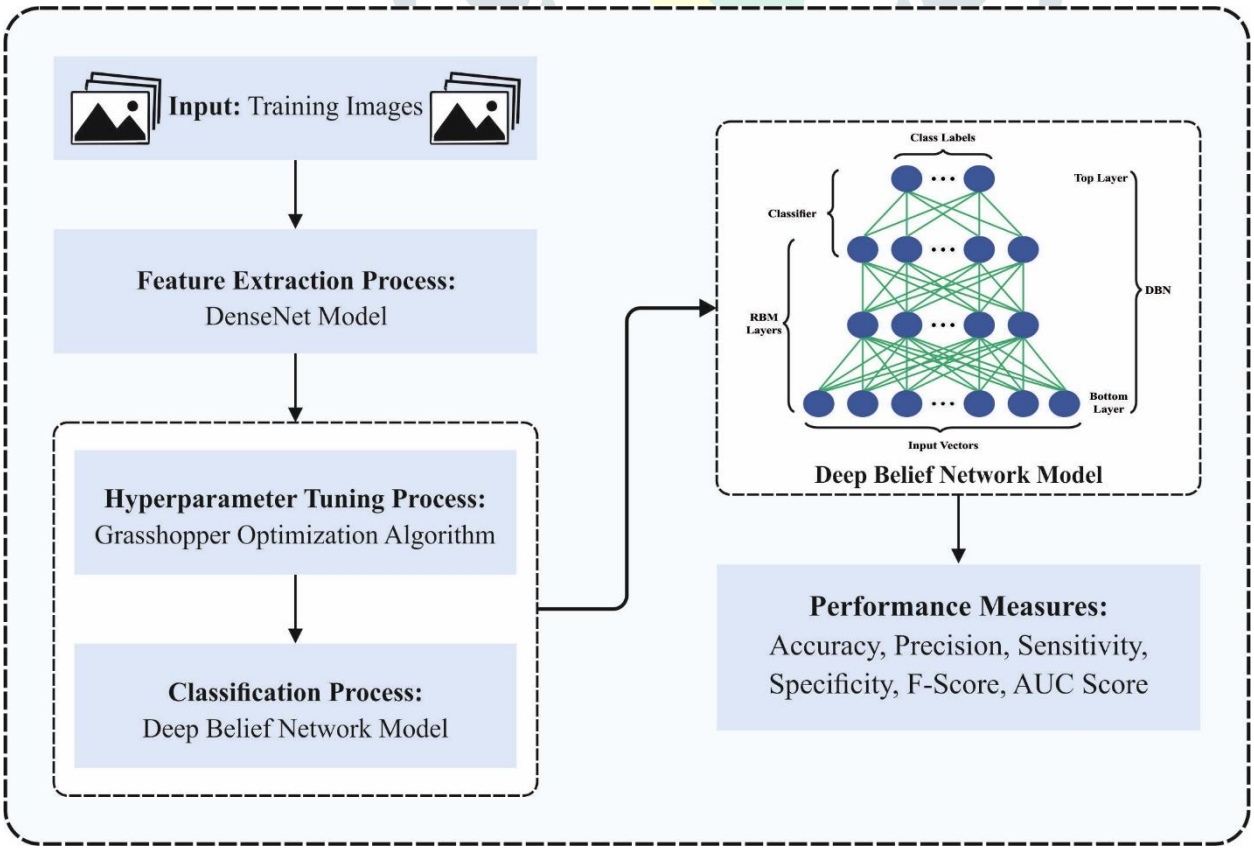

Fig. 1. Overall process of GOADL-BVSC algorithm

2.1. Feature extraction

For the process of feature extraction, DenseNet is employed in this study. DenseNet, short for Densely Connected Convolutional Network, is a deep learning model designed to address the gradient vanishing problems and enhance feature reuse in CNN [16]. In classical CNN, each layer is sequentially connected, and features are passed from one layer to the next. DenseNet introduces dense connection, where each layer is connected to each subsequent layer in a feedforward way. This dense connectivity allows gradient flow and feature propagation through short path, which mitigates the gradient vanishing problem. One of the considerable advantages of DenseNet is its parameter efficacy. Compared to classical architectures like ResNet, the number of parameters in the network is decreased due to dense connections. This enables more efficient training and better feature extraction. Moreover, DenseNet excels in feature reuse, as low-level features are easily accessible by deep layers, improving the model's representation ability. DenseNet architecture is commonly used for image segmentation, image classification, and object detection tasks. They have consistently accomplished state-of-the-art performance on benchmark datasets, which demonstrate the efficiency of dense connectivity in deep neural network.

2.2. Hyperparameter tuning

In this stage, the GOA is used for hyperparameter tuning process. GOA method is stimulated by the swarming and foraging behavior of grasshoppers in nature for finding numerical optimization problems [17]. The life cycle of the grasshopper comprises a 2 phases namely adulthood and nymph. Slight movements and small stages represent the nymph phase, whereas extensive and unexpected movements are considered the adulthood phase. Automatically expressing the GOA search method can be divided into 2 phases such as exploration and exploitation.

In the exploration phase, we update each the positions' values and calculate the fitness value of every grasshopper swarms (search for food sources). During exploitation phase, we determine the best solution between every solution (search for best food sources).

Principal of the GOA. In the GOA model, all grasshoppers describe a solution in the population. The grasshopper swarms behavior can be mathematically exhibited and employed for computing the position X_i of all solutions as given below:

$$X_i = S_i + G_i + A_i \tag{1}$$

Where S_i indicates the grasshopper interaction among the solutions and the other grasshoppers' swarms, x_i represents the ith grasshopper's position, A_i is the wind advection, and G_i indicates the gravity force on the ith solution that could be denoted by the given formula:

$$S_i = \sum_{j=1}^{N} s\left(d_{ij}\right)\widehat{d_{ij}}, \quad where\ i \neq j \tag{2}$$

$$s = fe^{\frac{-r}{l}} - e^{-r} \tag{3}$$

Where $d_{ij} = |x_j - x_i|$ describes the Euclidean distance among the ith and the jth grasshoppers swarm, N represents the number of grasshoppers, and $\widehat{d_{ij}} = \frac{|x_j - x_i|}{d_{ij}}$ signifies the unit vector from the ith to jth grasshopper swarm.

Additionally, s is the strength of 2 stages social forces (attraction and repulsion among grasshopper swarms), where f is the intensity of attraction and l is the attractive length scale. The mathematical formula indicates how to compute the force of gravity G_i:

$$G_i = -g\widehat{e_g} \tag{4}$$

Where $\widehat{e_g}$ is unit vector toward center of earth, g describes the gravitational constant and. The mathematical formula is given for how to calculate A_j:

$$A_i = u\widehat{e_w} \tag{5}$$

Where $\widehat{e_w}$ represents the unit vector in the wind direction, u is a drift constant and Then changing the values of S_i, G_i, and A_i, Eq. (1) could be regenerated succeeded by Eqs. (2), (3), (4) and (5):

$$X_i = \sum_{j=1}^{N} s\left(d_{ij}\right)\widehat{d_{ij}} - g\widehat{e_g} + u\widehat{e_w}$$

$$= \sum_{j=1}^{N} s\left(|x_j - x_j|\right)\frac{|\widehat{x_j - x_i}|}{d_{ij}} - g\widehat{e_g} + u\widehat{e_w}\ where\ i \neq j \tag{6}$$

Although, the mathematical form of Eq. (6) is not applied directly to determine the optimization issues, as primarily the grasshoppers rapidly reach their comfort situation and the grasshopper's swarms from failing to converge for locating target or certain point (global optimum). To determine optimization difficulties and avoid grasshopper swarms from rapidly attaining their comfortable zone, the calculation accurately utilized to find optimization issues are modelled by mathematical formula is gin:

$$X_i^d = c\left(\sum_{j=1}^{N} c\frac{UB_d - LB_d}{2} s\left(|x_j^d - x_i^d|\right)\frac{|x_j - x_i|}{d_{ij}}\right) + \widehat{T_d} \tag{7}$$

where LB_d and $UB_d$are the lower and upper boundaries in the dth dimension individually, $\overline{T_d}$ represent the best solution created so far in the dth dimension space. At Eq. (7), the gravity force could not measured without G_i constituent. And suppose that the wind direction (A_j component) has continually towards a target T_d. The second term $\widehat{T_d}$, regenerates the feature of grasshoppers to change towards the food source.

2.3. DBN based classification

At the final phase, the CVD classification method has been executed by employing DBN technique. DBN is a kind of artificial neural network that fuses the principle of deep learning and probabilistic graphical models [18].

DBNs comprise multiple layers of stochastic, hidden variables (nodes) that capture complex hierarchical representation of data. They are mainly utilized for unsupervised learning and have found applications in tasks such as generative modeling, feature learning, and dimensionality reduction. The architecture of DBN generally includes a stack of Restricted Boltzmann Machines (RBMs), which are a kind of probabilistic graphical model. Each RBM comprises of two layers: a visible layer representing the observed data and hidden layer that models hidden variables. RBM is trained by a contrastive divergence model that adjusts the weight to maximize the probability of the observed data. The strength of DBNs lies in their capability to automatically learn hierarchical features from raw information. This hierarchical feature learning enables them to capture intricate patterns and dependency in complex datasets, making them suitable for tasks like image and speech recognition. Also, DBN is finetuned for supervised learning task by adding additional output layer, transforming them into DBNs. One of the significant benefits of DBNs is their capability to effectively initialize deep neural network. By pretraining each layer as an RBM and finetuning the entire network, DBNs alleviate the gradient vanishing problems, enabling the training of deep architecture. This pretraining model has been pivotal in the success of deep learning in various fields.

3. Experimental validation

The proposed GOADL-BVSC system is tested employing the DR database from Kaggle repository [19]. The database holds 35126 instances with five classes as described in Table 1.

Table 1 Details of DR dataset

Label	**Class**	**No. of Instances**
DR-0	No DR	25810
DR-1	Mild DR	2443
DR-2	Moderate DR	5292
DR-3	Severe DR	873
DR-4	Proliferative DR	708
Total Number of Instances		**35126**

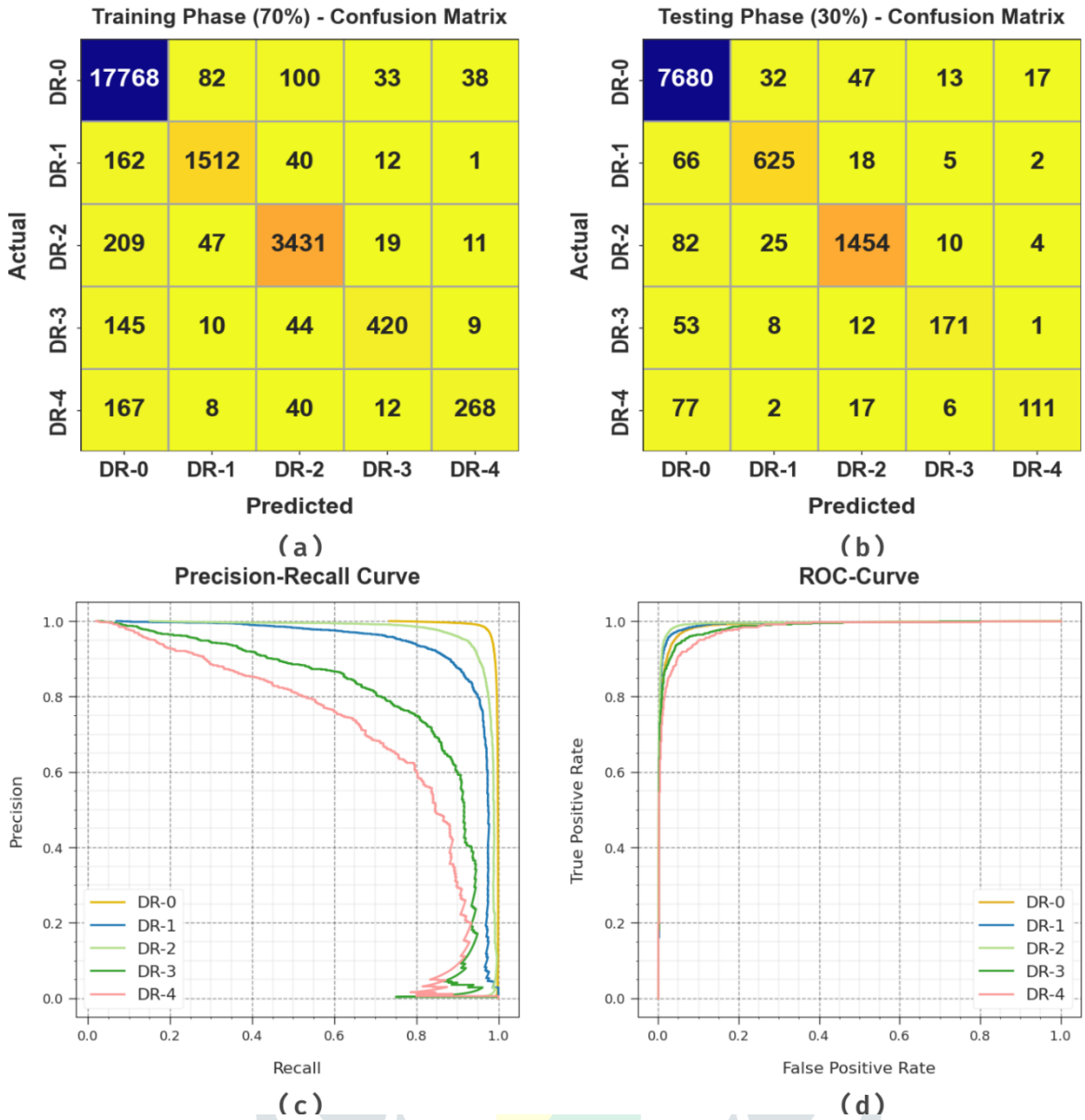

Fig. 2. Classifier performance (a-b) Confusion matrices, (c) PR curve, (d) ROC

Fig. 2 shows the classifier analysis of the GOADL-BVSC system on the test database. Figs. 2a-2b represents the confusion matrices offered by the GOADL-BVSC technique at 70:30 of TR phase/TS phase. The figure indicated that the GOADL-BVSC model has precisely identified and categorized all 5 classes. Additionally, Fig. 2c exhibits the PR analysis of the GOADL-BVSC approach. The figure shows that the GOADL-BVSC model has attained better PR performance with each classes. Lastly, Fig. 2d illustrates the ROC analysis of the GOADL-BVSC methodology. The figure represented that the GOADL-BVSC technique can be effective outcomes with superior ROC values with each class.

Table 2 exhibits the DR classification analysis of GOADL-BVSC system at 70:30 of TR phase/TS phase. The simulated outcome indicates that the GOADL-BVSC algorithm proficiently detects with each class. Additionally, based on 70% of TR phase, the GOADL-BVSC methodology attains average $accu_y$, $prec_n$, $sens_y$, $spec_y$, and F_{score} of 98.07%, 89.59%, 79.89%, 97.46%, and 83.95%. Likewise, with 30% of TS phase, the GOADL-BVSC approach gets average $accu_y$, $prec_n$, $sens_y$, $spec_y$, and F_{score} of 98.11%, 89.28%, 80.02%, 97.52%, and 83.85% respectively.

Table 2 DR classifier outcome of GOADL-BVSC approach with 70:30 of TR phase/TS phase

Class	Accuracy	Precision	Sensitivity	Specificity	F-Score
Training Phase (70%)					
DR-0	96.19	96.30	98.60	89.60	97.43
DR-1	98.53	91.14	87.55	99.36	89.31
DR-2	97.93	93.87	92.31	98.93	93.08
DR-3	98.84	84.68	66.88	99.68	74.73
DR-4	98.84	81.96	54.14	99.76	65.21
Average	**98.07**	**89.59**	**79.89**	**97.46**	**83.95**
Testing Phase (30%)					
DR-0	96.33	96.51	98.60	89.89	97.54
DR-1	98.50	90.32	87.29	99.32	88.78
DR-2	97.96	93.93	92.32	98.95	93.12
DR-3	98.98	83.41	69.80	99.67	76.00
DR-4	98.80	82.22	52.11	99.77	63.79
Average	**98.11**	**89.28**	**80.02**	**97.52**	**83.85**

Table 3 and Fig. 3 illustrates the comparison outcome of GOADL-BVSC technique with other systems for $accu_y$. The simulated value inferred that the GOADL-BVSC method attain efficacious outcomes. According to $accu_y$, the GOADL-BVSC methodology has surpassed greater value with $accu_y$ of 98.11%, whereas the AlexNet, VGG-16, ResNet-50, ResNet-101, and Inception V3 systems are indicated minimum values with $accu_y$ of 88.81%, 95.98%, 92.95%, 93.88%, and 95.10% correspondingly.

Table 3 $Accu_y$ outcome of GOADL-BVSC approach with other methods

Methods	Accuracy
AlexNet Model	88.81
VGG-16 Model	95.98
ResNet-50 Model	92.95
ResNet-101 Model	93.88
Inception V3 Model	95.10
GOADL-BVSC	98.11

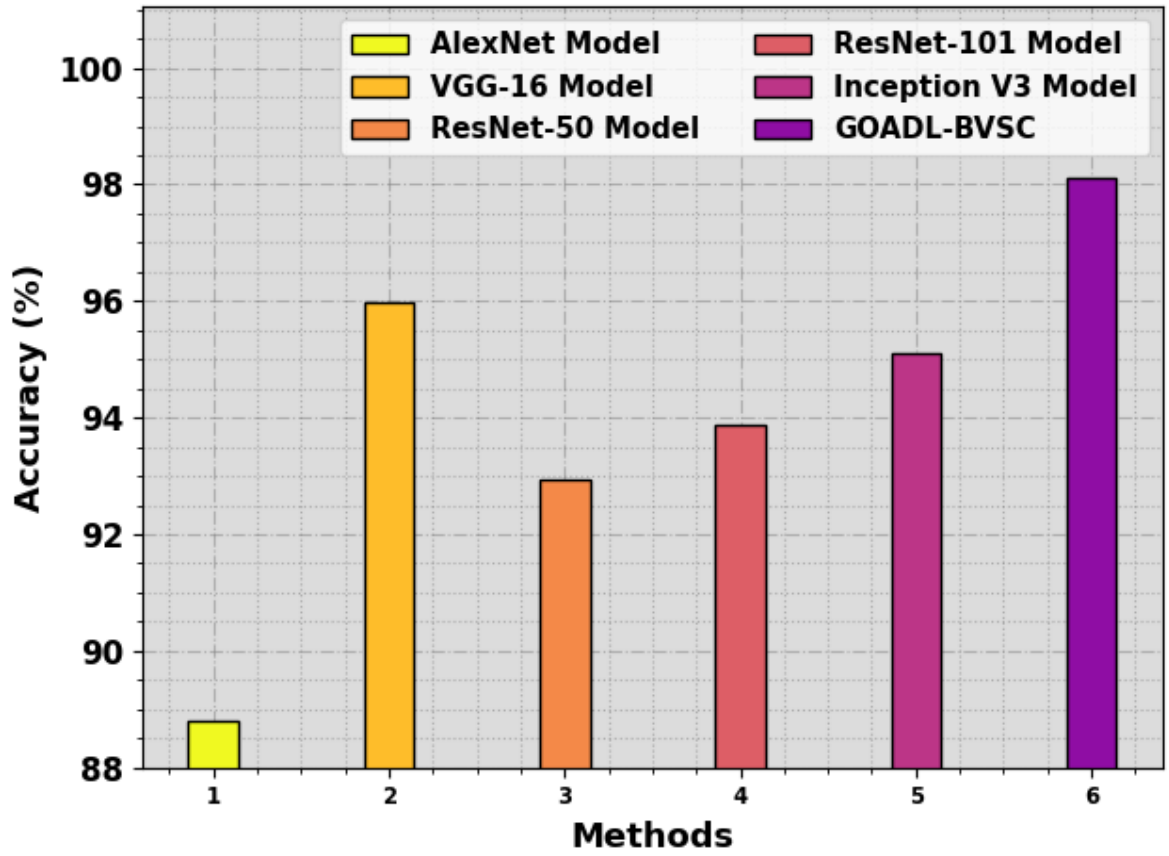

Fig. 3. $Accu_y$ outcome of GOADL-BVSC approach with other methods

Table 4 describes the details of CVD dataset. The dataset comprises 400 samples with a 2 classes.

Table 4 Details of CVD dataset

Class	**No. of Samples**
CVD_Positive	200
CVD_Negative	200
Total Samples	**400**

Fig. 4 shows the classifier analysis of the GOADL-BVSC system with test database. Figs. 4a-4b illustrates the confusion matrices given by the GOADL-BVSC system at 70:30 of TR phase/TS phase. The figure signified that the GOADL-BVSC approach has appropriately identified and categorized all 2 classes. Moreover, Fig. 4c represents the PR analysis of the GOADL-BVSC technique. The figure stated that the GOADL-BVSC algorithm has attained better PR performance with each class. Besides, Fig. 4d shows the ROC analysis of the GOADL-BVSC methodology. The figure revealed that the GOADL-BVSC system leads to effective outcome with higher ROC values with each class.

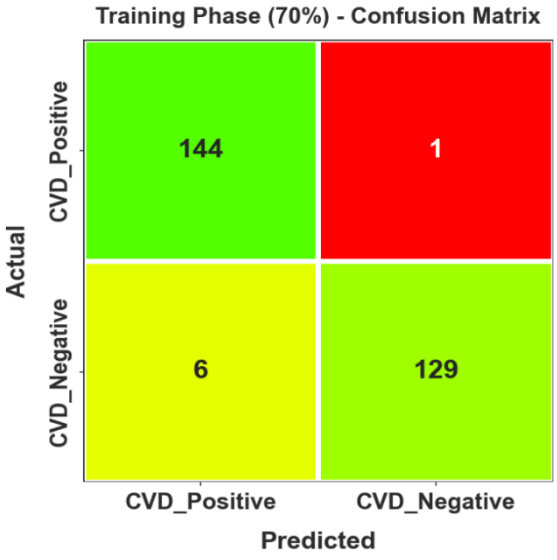
Training Phase (70%) - Confusion Matrix
Actual
CVD_Positive
CVD_Negative
144
1
6
129
CVD_Positive
CVD_Negative
Predicted

(a)

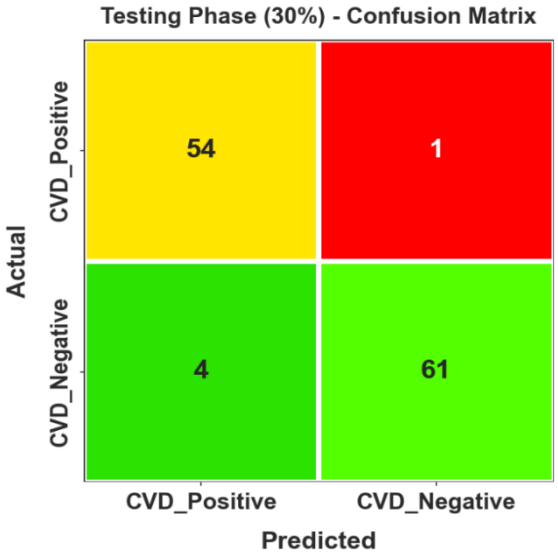
Testing Phase (30%) - Confusion Matrix
Actual
CVD_Positive
CVD_Negative
54
1
4
61
CVD_Positive
CVD_Negative
Predicted

(b)

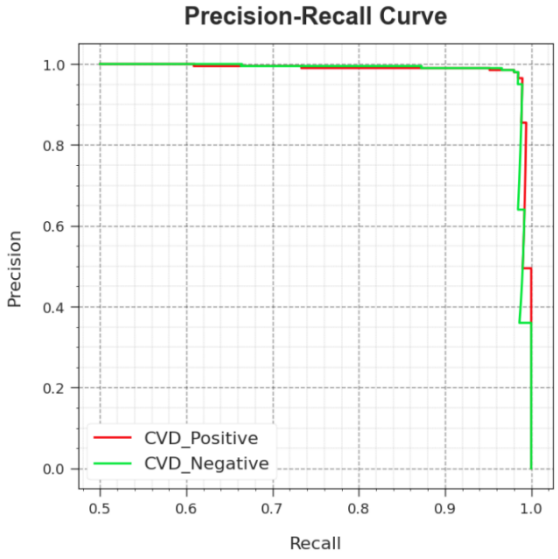
Precision-Recall Curve
Precision
Recall
CVD_Positive
CVD_Negative

(c)

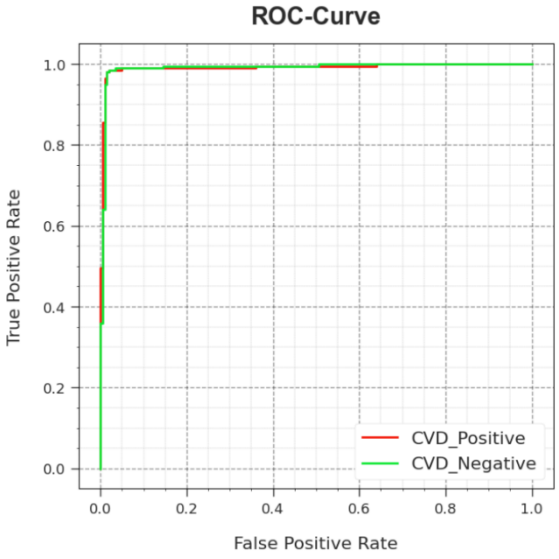
ROC-Curve
True Positive Rate
False Positive Rate
CVD_Positive
CVD_Negative

(d)

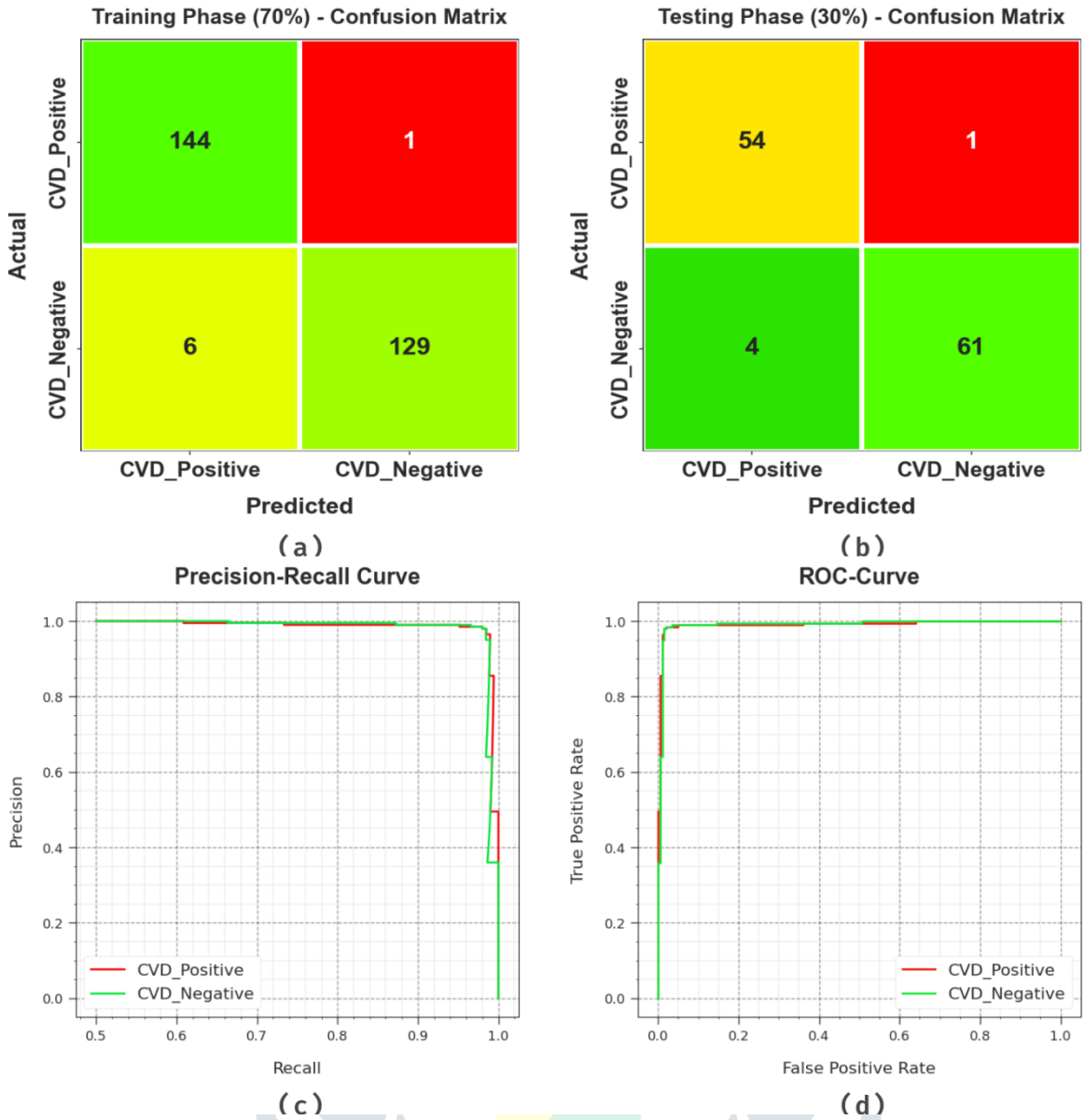

Fig. 4. Classifier performance (a-b) Confusion matrices, (c) PR curve, (d) ROC

Table 5 illustrates the CVD classification analysis of GOADL-BVSC method at 70:30 of TR phase/TS phase. The simulated outcome denotes that the GOADL-BVSC technique efficiently detects all 2 classes. According to 70% of TR phase, the GOADL-BVSC system gets average $accu_y$, $prec_n$, $sens_y$, $spec_y$, and AUC_{score} of 97.43%, 97.62%, 97.43%, 97.43%, and 97.49%. Likewise, based on 30% of TS phase, the GOADL-BVSC methodology acquires average $accu_y$, $prec_n$, $sens_y$, $spec_y$, and AUC_{score} of 96.01%, 95.75%, 96.01%, 96.01%, and 95.82% respectively.

Table 5 CVD classifier outcome of GOADL-BVSC approach with 70:30 of TR phase/TS phase

Class	Accuracy	Precision	Sensitivity	Specificity	AUC Score
Training Phase (70%)					
CVD_Positive	99.31	96.00	99.31	95.56	97.63
CVD_Negative	95.56	99.23	95.56	99.31	97.36
Average	**97.43**	**97.62**	**97.43**	**97.43**	**97.49**
Testing Phase (30%)					
CVD_Positive	98.18	93.10	98.18	93.85	95.58
CVD_Negative	93.85	98.39	93.85	98.18	96.06
Average	**96.01**	**95.75**	**96.01**	**96.01**	**95.82**

Table 6 and Fig. 5 represents the comparison analysis of GOADL-BVSC technique with other approaches with respect to $accu_y$ [20, 21]. The simulated outcome exhibits that the GOADL-BVSC model attain successful outcomes. Also, with $accu_y$, the GOADL-BVSC system has exceeded better value with $accu_y$ of 97.43%, whereas the Inception-ResNet-V2, U-Net-VGG19, Inception V3, and CNN-ResNet50 methodologies are represented as decreased values with $accu_y$ of 97%, 96%, 91%, and 80% correspondingly.

Table 6 $Accu_y$ outcome of GOADL-BVSC approach with other methods

Architectures	Accuracy (%)
GOADL-BVSC	97.43
Inception-ResNet-V2	97.00
U-Net-VGG19	96.00
InceptionV3	91.00
CNN-ResNet50	80.00

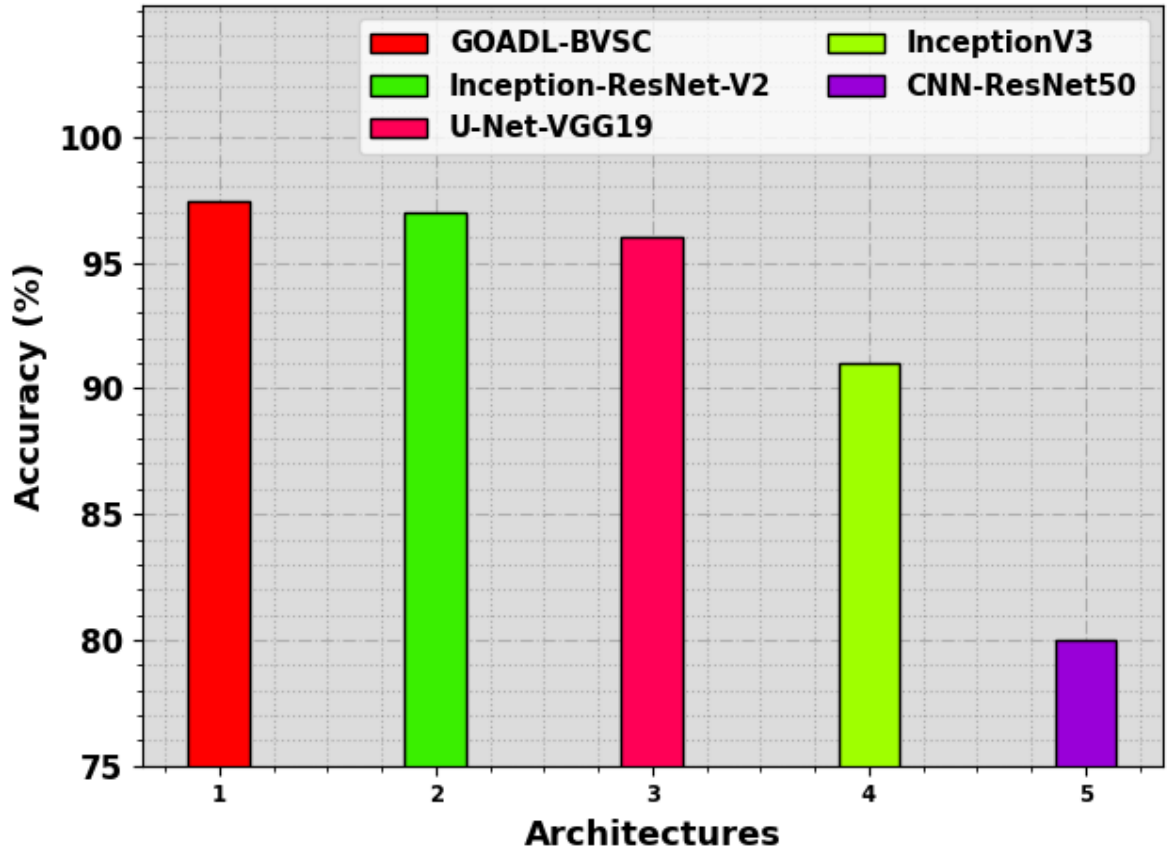

Fig. 5. $Accu_y$ outcome of GOADL-BVSC approach with other methods

4. Conclusion

In this study, we present an innovative GOADL-BVSC model for grading the CVD. This analysis suggests a robust method for CVD detection by connecting DL methodologies, particularly utilizing DenseNet for feature extraction, GOA for parameter tuning, and DBN for classification. Retinal fundus images provide useful resources for evaluating cardiovascular conditions, giving a non-invasive and quickly accessible process of detecting CVDs. GOA iteratively enhances the hyperparameters of the DBN, confirming that the system attains its maximum

accuracy capability. The simulation outcomes represented the excellent outcomes of the GOADL-BVSC method over other existing models with regard to different levels.

References

[1] Schmarje, L.; Santarossa, M.; Schröder, S.M.; Koch, R. A survey on semi-, self-and unsupervised learning for image classification. IEEE Access 2021, 9, 82146–82168.

[2] Van Engelen, J.E.; Hoos, H.H. A survey on semi-supervised learning. Mach. Learn. 2020, 109, 373–440.

[3] Simonyan, K.; Zisserman, A. Very deep convolutional networks for large-scale image recognition. arXiv 2014, arXiv:1409.1556.

[4] Abdullah, M.; Fraz, M.M.; Barman, S.A. Localization and segmentation of optic disc in retinal images using circular Hough transform and grow-cut algorithm. PeerJ 2016, 4, e2003.

[5] Ambale-Venkatesh B, Yang X, Wu CO, et al. Cardiovascular Event Prediction by Machine Learning: The Multi-Ethnic Study of Atherosclerosis. Circ Res. 2017;121:1092–1101.

[6] Alaa AM, Bolton T, Di Angelantonio E, Rudd JHF, van der Schaar M. Cardiovascular disease risk prediction using automated machine learning: A prospective study of 423,604 UK Biobank participants. PLoS One. 2019.

[7] Mitani A, Huang A, Venugopalan S, et al. Detection of anaemia from retinal fundus images via deep learning. Nature Biomedical Engineering. 2020;4:18–27.

[8] de Carlo TE, Chin AT, Bonini Filho MA, et al. Detection of microvascular changes in eyes of patients with diabetes but not clinical diabetic retinopathy using optical coherence tomography angiography. Retina. 2015;35:2364–2370.

[9] Thompson IA, Durrani AK, Patel S. Optical coherence tomography angiography characteristics in diabetic patients without clinical diabetic retinopathy. Eye. 2019;33:648–652.

[10] Chamnan P, Simmons RK, Sharp SJ, et al. Cardiovascular risk assessment scores for people with diabetes: a systematic review. Diabetologia 2009;52:2001–14.

[11] Schlesinger, D.E. and Stultz, C.M., 2020. Deep learning for cardiovascular risk stratification. *Current Treatment Options in Cardiovascular Medicine*, *22*, pp.1-14.

[12] Revathi, T.K., Sathiyabhama, B. and Sankar, S., 2021. Diagnosing cardio vascular disease (CVD) using generative adversarial network (GAN) in retinal fundus images. *Annals of the Romanian Society for Cell Biology*, pp.2563-2572.

[13] Srilakshmi, V., Anuradha, K. and Bindu, C.S., 2022. Intelligent decision support system for cardiovascular risk prediction using hybrid loss deep joint segmentation and optimized deep learning. *Advances in Engineering Software*, *173*, p.103198.

[14] Cho, S., Song, S.J., Lee, J., Song, J., Kim, M.S., Lee, M. and Lee, J., 2020. Predicting coronary artery calcium score from retinal fundus photographs using convolutional neural networks. In *Artificial Intelligence and Soft Computing: 19th International Conference, ICAISC 2020, Zakopane, Poland, October 12-14, 2020, Proceedings, Part I 19* (pp. 599-612). Springer International Publishing.

[15] Rim, T.H., Lee, C.J., Tham, Y.C., Cheung, N., Yu, M., Lee, G., Kim, Y., Ting, D.S., Chong, C.C.Y., Choi, Y.S. and Yoo, T.K., 2021. Deep-learning-based cardiovascular risk stratification using coronary artery calcium scores predicted from retinal photographs. *The Lancet Digital Health*, *3*(5), pp.e306-e316.

[16] Cao, Y., Liu, S., Peng, Y. and Li, J., 2020. DenseUNet: densely connected UNet for electron microscopy image segmentation. *IET Image Processing*, *14*(12), pp.2682-2689.

[17] Wu, L., Wu, J. and Wang, T., 2023. Enhancing grasshopper optimization algorithm (GOA) with levy flight for engineering applications. *Scientific Reports*, *13*(1), p.124.

[18] Zhang, Y., Ji, J. and Ma, B., 2020. Fault diagnosis of reciprocating compressor using a novel ensemble empirical mode decomposition-convolutional deep belief network. *Measurement*, *156*, p.107619.

[19] https://www.kaggle.com/competitions/diabetic-retinopathy-detection/overview

[20] Barriada, R.G. and Masip, D., 2022. An Overview of Deep-Learning-Based Methods for Cardiovascular Risk Assessment with Retinal Images. *Diagnostics*, *13*(1), p.68.

[21] Nneji, G.U.; Cai, J.; Deng, J.; Monday, H.N.; Hossin, M.A.; Nahar, S. Identification of Diabetic Retinopathy Using Weighted Fusion Deep Learning Based on Dual-Channel Fundus Scans. Diagnostics 2022, 12, 540. https:// doi.org/10.3390/diagnostics12020540